

Target Thermal Response to Gas Interactions

A. R. Raffray, J. Pulsifer and M. S. Tillack

June 24, 2002



**Fusion Division
Center for Energy Research**

University of California, San Diego
La Jolla, CA 92093-0417

Target Thermal Response to Gas Interactions

A. R. Raffray, J. Pulsifer and M. S. Tillack
Jacobs School of Engineering and the Center for Energy Research
University of California, San Diego

June 24, 2002

ABSTRACT

Detailed analysis of convection heat transfer and gas condensation on direct drive targets has been performed in order to provide a more accurate estimate of the temperature rise. Transient analysis of the target thermal response was performed near the triple point using DT properties corresponding to each phase. The calculations provide better insight into the knee in the maximum temperature curve. As compared with previous estimates, lower allowable heat flux is predicted as the triple point is reached. Careful examination of gas transport near the target surface indicates that shielding of the incident particle flux by uncondensed gas is important for pressures greater than 1 mtorr. Therefore, more accurate treatment of particle sticking must be used. High sticking coefficients will lower the allowable gas temperature and pressure in the chamber.

1. Introduction

Direct drive targets are relatively delicate due to the lack of protection against the high-temperature chamber environment and the stringent requirements on implosion symmetry. The design window is tight. Uncertainties remain in the appropriate design goals, basic property data, and modeling of interactions with the chamber constituents. The uncertainties are larger than the design window, such that successful target injection into the chamber can not be assured. Below we report initial results of detailed thermal analysis of direct drive target including convection and condensation heat transfer from the surrounding gas. Differences with previous estimates are highlighted.

The reference target is shown in Figure 1. It consists of a ~ 4 mm diameter spherical shell composed mainly of solid deuterium-tritium (DT) at a temperature of 18 K. The target is injected at velocities up to about 400 m/s in an IFE chamber of typical size ~ 6 m.

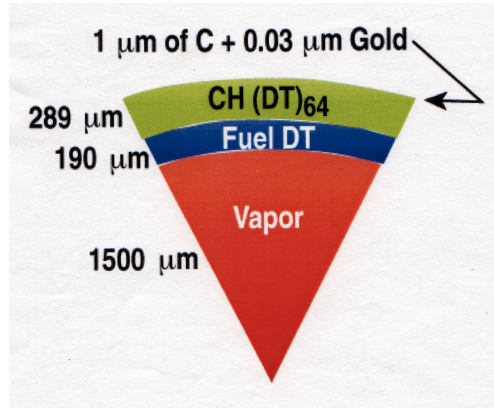


Figure 1. Diagram of the layers in a spherical direct-drive target.

Heat transfer to the target is important because the target can deform due to thermal stresses or phase change in the DT. Deformation of the outer layer of target material can greatly affect the target gain and possibly prevent the target from igniting. Although it is not clear what the maximum temperature limit is to prevent unacceptable target outer layer deformation it has been assumed that the target surface temperature should be maintained below the triple point of DT (19.79 K). Thus, the temperature increase of the target during flight to the center of the chamber should be lower than 1.79 K for an 18 K initial target temperature.

An important component of the heat transfer to the target is associated with the transfer of energy from the impinging background gas (such as xenon), which might be needed in the chamber for wall protection and through which the target must travel. The background gas would condense on the target surface thereby heating it up. In addition, if plasma conditions remain, recombination of ions at the surface would result in even larger heat transfer. However, it is not clear what would be the plasma conditions and this initial report focuses on the effect of condensation of Xe as background gas on the target.

Another important heat transfer mechanism is radiation from the chamber wall. It has been addressed to some level before [1] and has been shown to be of potential concern depending on

the surface reflectivity. However, the results are highly dependent on the analysis procedure and on the assumed optical properties of the target constituents. This is the subject of further investigations and will be covered in a later report.

2. Direct Simulation Monte Carlo Model for Heat Flux

Convection heat transfer from the background gas to the target has been analyzed previously over different regimes (molecular, transition and continuity) but without explicitly considering condensation [1]. For the 4-mm target case, the transition regime (Knudsen number =0.1) applies for Xe pressure of about 100 mtorr (at 300 K) or lower and the full molecular regime for Xe pressure of ~1 mtorr (at 300 K) or lower. These include the range of pressures anticipated for a direct drive target with a dry wall; clearly continuum regime convection heat transfer would not apply. For this reason we decided to use a direct simulation Monte Carlo (DSMC) program to determine the heat flux at the surface of an IFE target consistent with prior analysis at GA [2].

Figure 2 shows an example result of the DSMC heat flux calculations for a background Xe temperature of 4,000 K and density corresponding to a pressure of 10 mtorr at 300 K (this measure has been used for some time as a typical way to represent the Xe density). The heat flux varies along the surface of the target, with the maximum heat flux at the leading edge of the target (trailing edge is at 0 in Figure 2). For ease of computation, the DSMC model assumed a sphere diameter of 40 cm and the effective Xe density used in the calculations is set 100 times lower than the actual target case (based on the diameter ratio) so as to maintain the same Knudsen number. The DSMC heat flux results then must be multiplied by 100 to obtain the actual target heat flux. For example, the maximum heat flux shown in Figure 2 is ~200 W/m² for the 40 cm diameter DSMC model, from which the corresponding maximum heat flux on a 4 mm target with the same Knudsen number would be ~20,000 W/m².

For each Xe case analyzed, the heat flux distribution over the target surface obtained from the DSMC calculations (as illustrated in Figure 2) was used to calculate the maximum target temperature from a 2-D transient thermal analysis utilizing the ANSYS finite element code [3]. The maximum temperature is assumed to occur when the target reaches the center of the chamber,

which, for a 400 m/s target in a 6-m radius chamber, corresponds to a flight time of 0.015 s. In all cases the heat flux distribution could be reasonably represented by two straight line fits (within ~10%) and, for simplicity, this was used in these initial calculations. DT property data from Ref. [1] were used for these calculations.

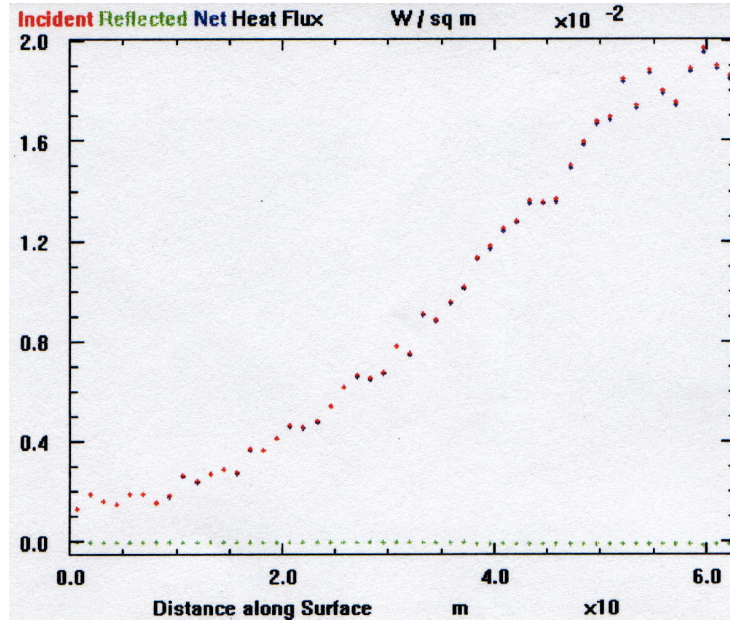


Figure 2. DSMC heat flux result for a 400 m/s target injected through Xe at a temperature of 4,000 K and a density corresponding to 10 mtorr at 300 K.

Figure 3 shows the target temperature distribution after 0.015 s for a case with Xe at a temperature of 4,000 K and a density corresponding to 10 mtorr at 300 K. The temperature rise at the leading edge is 2.388 K, which is unacceptable based on our assumptions since the triple point of DT has been exceeded.

Figure 4 summarizes the results of the DSMC/ANSYS calculations for a velocity of 400 m/s. The computations span Xe temperatures from 1,000 to 4,000 K and pressures (at 300 K) from 1 to 100 mtorr. The figure shows the maximum temperature change of the target as a function of the maximum heat flux at the target surface for 3 different chamber radii (affecting the time of flight for a given injection velocity). The ANSYS model assumes that the target is not tumbling, i.e. the same side of the target is always facing forward. Therefore, the leading edge of the target is exposed to the maximum heat flux during the entire time of flight. The temperature change of the target increases in a linear fashion up to the triple point of DT. At the triple point, there is a

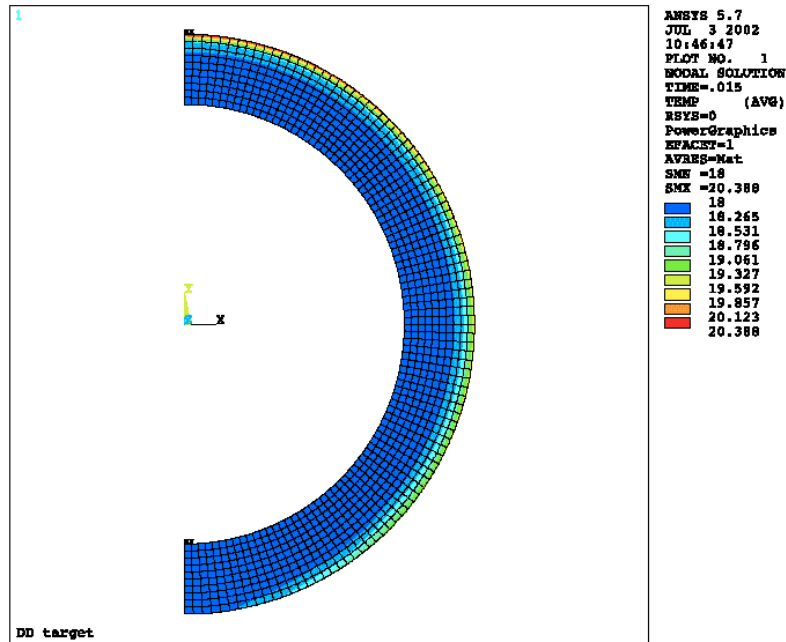


Figure 3. ANSYS solution using heat flux from the DSMC results shown in Fig 2. (Initial target temperature = 18 K, time of flight = 0.015 s. T_{max} = 20.388 K)

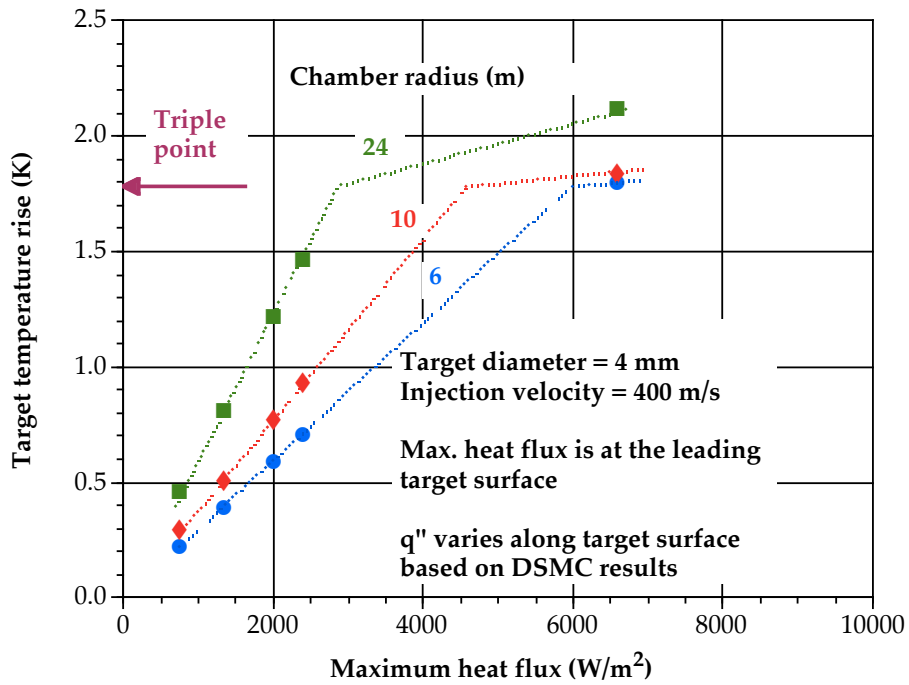


Figure 4. Summary of ANSYS results at 400 m/s.

knee in the curve where additional heat flux does not affect the temperature as much, consistent with the phase change when going from solid to liquid DT. From the figure, the heat flux to reach the triple point is about 6000 W/m² for a 6-m radius chamber and even lower for larger chambers.

Figure 5 shows the maximum heat flux (from DSMC) as a function of the Xe pressure (at room temperature, 300 K) for four different Xe temperatures. Even with Xe at 1,000 K, the target is heated to the triple point with a Xe background pressure of only ~10 mtorr.

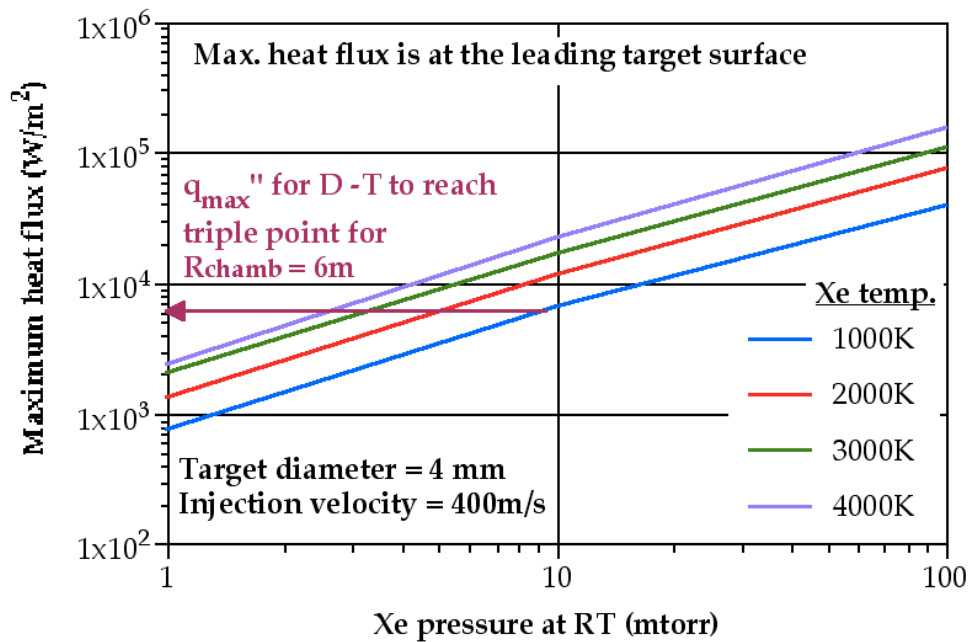


Figure 5. Maximum heat flux on the target as a function of Xe pressure at RT for different Xe temperatures (from DSMC).

The DSMC computations of the heat flux assume that the temperature of the impinging Xe atoms drops to 18 K, but that no Xe atoms stick to the target surface. Rather, they drop in temperature and then reflect from the surface where they provide a shield against subsequent atom collisions. However, depending on the condensation coefficient, a significant fraction of Xe atoms could stick to the target surface thereby not shielding subsequent atom collisions and resulting in higher, more challenging heat fluxes on the target. A condensation analysis was done to assess this possibility.

3. Condensation Analysis

The Xe condensation flux, j_{cond} can be calculated as follows using expression for the mass flow rate of Xe molecules (based on the actual Xe pressure, P_{Xe} , and temperature, T_{Xe} ,) and a condensation coefficient, β_c [3]:

$$j_{cond}(\pm a) = \sqrt{\frac{M}{2\pi R}} \cdot \beta \cdot \beta_c \frac{P_{Xe}}{\sqrt{T_{Xe}}} \quad (1)$$

where M is the molecular weight of Xe and R is the universal gas constant. In addition, a correction factor, β , is used to account for the effect of Xe velocity respective to the target surface [3]. A characteristic velocity, v_{char} , is first calculated as follows:

$$v_{char} = \sqrt{2R_{Xe}T_{Xe}} \quad (2)$$

$$\text{where: } R_{Xe} = \frac{\bar{R}}{M_{Xe}} \quad (3)$$

A dimensionless velocity is defined as:

$$a = \frac{v_{target}}{v_{char}} \quad (4)$$

where v_{target} is the injection velocity (~400 m/s)

The correction factor, β , is calculated from the following expressions for cases where the velocity is toward (+a) and away from (-a) the surface, respectively:

$$\beta(a) = \exp(-\beta a^2) + a\sqrt{\beta}[1 + \text{erf } a] \text{ (leading edge gamma)} \quad (5)$$

$$\beta(-a) = \exp(-\beta a^2) - a\sqrt{\beta}[1 - \text{erf } a] \text{ (trailing edge gamma)} \quad (6)$$

the actual Xe pressure is given by:

$$P_{Xe} = \frac{P_{300,Xe} T_{Xe}}{300} \quad (7)$$

The heat flux at the target surface, q'' , is calculated as follows for $j_{cond}(\pm a)$:

$$q''(\pm a) = j_{cond} \left[c_p (T_{Xe} - T_{target}) + h_{fg} + h_s \right] \quad (8)$$

where c_p is the specific heat of Xe and h_{fg} and h_s are the latent heats of vaporization and fusion of Xe, respectively (listed in Table 1). The maximum heat flux, q''_{max} , occurs at the leading edge, $q''(+a)$.

Table 1. Properties of Xe and He

Properties	Xe	He
Molecular weight	131.1	4
Melting point (K)	161.36	0.95
Boiling point (K)	165.03	4.22
Specific heat capacity, Cp (J/kg-K)	~158.3	~5192
Latent heat of vaporization, h_{fg} (J/kg)	9.62×10^4	2.08×10^4
Latent heat	1.71×10^4	5000

of fusion, h_s (J/kg)		
----------------------------	--	--

Figure 6 illustrates the results in term of the maximum condensation heat flux as a function of the product of Xe pressure and condensation coefficient ($\bar{\alpha}_c P_{Xe}$) for cases with different Xe temperatures and injection velocities. These results for q''_{max} are consistent with those from DSMC runs (Fig. 5) for condensation coefficients, $\bar{\alpha}_c$'s, ranging from ~ 0.5 at 100 mtorr to ~ 1 at 1 mtorr. This is consistent with the assumptions used in DSMC as for very low pressure shielding of subsequent atom collisions by atoms reflecting from the surface would be minimal (with $\bar{\alpha}_c = 1$ from the corresponding condensation analysis) whereas shielding is more effective as the Xe pressure increases (with correspondingly lower $\bar{\alpha}_c$'s from the condensation analysis).

It is not clear what the condensation coefficient is for Xe at $\sim 1,000$'s K condensing on an 18 K surface since no data were found for this specific case. However, experimental data from Ref. [4] indicate $\bar{\alpha}_c$ values of 0.99-0.6 for 2,500 K Ar beam condensing on an 15 K Cu/Ar with incident angle of 0° - 60° . These high values of $\bar{\alpha}_c$ are of concern since from this analysis they could result in the target surface exceeding the triple point even with low Xe pressure.

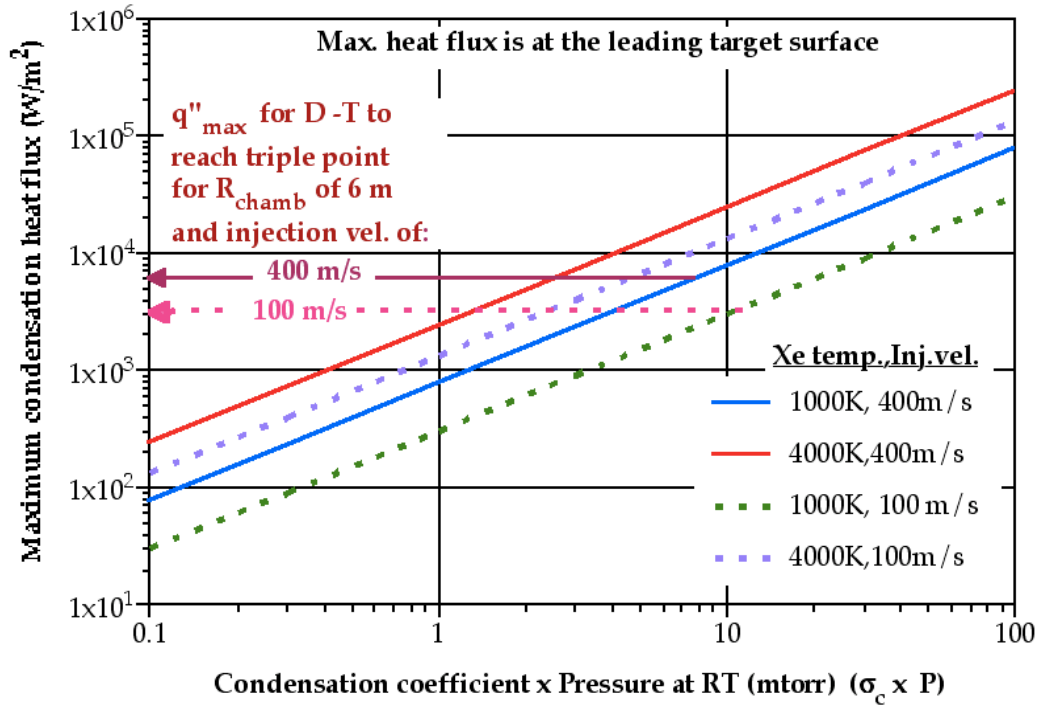


Figure 6. Maximum condensation heat flux as a function of $(\bar{\Gamma}_c P_{Xe})$ for cases with different Xe temperatures and injection velocities.

Table 2 shows the combinations of $\bar{\Gamma}_c \cdot P_{Xe}$ and T_{Xe} that would cause the target surface to reach the triple point (from the results shown in Fig. 5). For a $\bar{\Gamma}_c$ close to unity for normal ion incidence, even for a case with a low Xe temperature of 1000 K and a velocity of 100 m/s, the Xe pressure would be limited to about 10 mtorr to avoid reaching the triple point. This would place an important constraint on background gas density that might be required for wall protection.

Table 2. Combination of parameters to reach triple point

v_{target} (m/s)	$\bar{\Gamma}_c \cdot P_{Xe}$ (mtorr)	T_{Xe} (K)
400	7.6	1,000
400	2.5	4,000
100	11	1,000
100	2.4	4,000

One way of reducing the condensation heat flux on the target could be to use a different background gas which must also be compatible with driver and chamber wall design and operation. Helium would be a good choice as it is an inert gas which is already present in the chamber as a product of the fusion reaction. It also has low boiling and melting points (see Table 1) which means that its latent heats of fusion and vaporization will not contribute to the energy transfer to ~18 K targets. Calculations were done to estimate the heat fluxes on the target from energy transfer from He atoms at different pressures and temperatures. The results are illustrated in Figure 7.

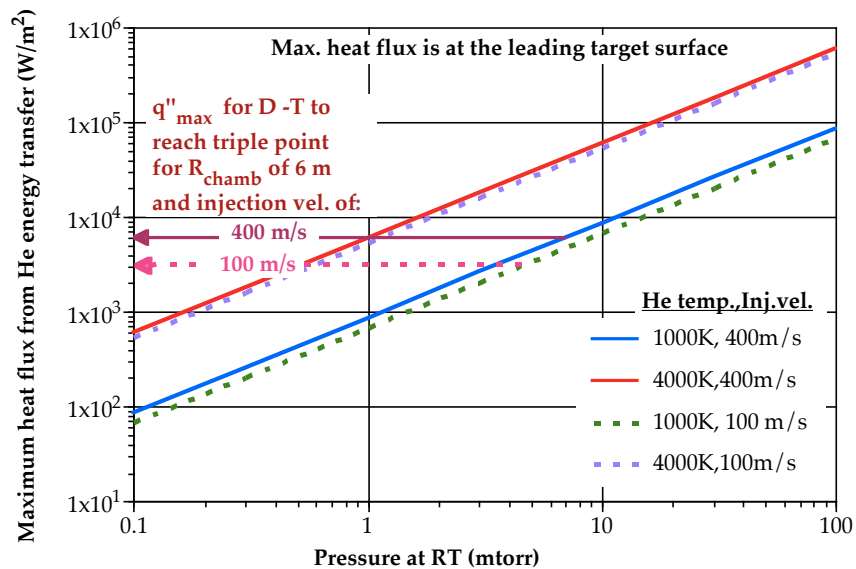


Figure 7. Maximum heat flux from He energy transfer as a function of He pressure at room temperature for cases with different He temperatures and injection velocities.

As shown in the figure, the heat fluxes on the target were found to be actually higher than those from the Xe case, which can be explained as follows: (1) the latent heats have only a small effect on the overall energy transfer which is mostly governed by the change in the gas heat capacity (see Table 1); and (2) the molecular flux of He on the moving target are higher than those of Xe for the same pressure and temperature as estimated from Eq. (1). However, use of He has the advantage that the He atoms after transferring their energy to the 18 K target will likely be

reflected back thereby shielding the target from subsequent He atom collisions. This is similar to what was assumed for the Xe DSMC calculations (see Section 2) and would reduce the heat transfer in particular for the higher He density cases. However, the heat flux on the target is not expected to be significantly lower than what was estimated for the Xe case.

4. Conclusions and Recommendations

A detailed condensation analysis for the direct drive target has been performed including the effect of the condensation coefficient. Prior analysis using DSMC had assumed that the Xe background gas atoms would deposit all their energy on the target but would be reflected at the target temperature. As shown in this report, this tended to be inaccurate for higher Xe pressure cases (> 1 mtorr at 300 K) as the reflected atoms would partly shield the target from subsequent atom collisions. The analysis shows that the values of the maximum condensation heat flux are consistent with those from DSMC runs for condensation coefficients ranging from ~ 0.5 at 100 mtorr to ~ 1 at 1 mtorr.

It is not clear what is the thermal limit of the target. Because of concern with phase change and potential surface deformation, the DT triple point was used as a limit. A better estimate of the maximum target temperature rise based on the maximum heat flux was done using a 2-D ANSYS transient analysis and using DT properties corresponding to each phase. The calculations were done over a broad range to provide a better insight on the knee in the maximum temperature curve as the triple point is reached. This has enabled a better estimate of the maximum allowable heat flux, which is lower than previously estimated. For example, for an 18 K direct drive target injected at 400 m/s in a 6-m radius chamber the maximum heat flux for the target to reach the triple point is 6000 W/m^2 .

A condensation heat flux of 6000 W/m^2 would be achieved by a combination of Xe at less than $\sim 10^{-4}$ mtorr (at 300 K) depending on the condensation coefficient. Thus, even based solely on Xe condensation, target heating is a major issue (depending on β_c) if a protective gas with adequate density is required (~ 10 's of mtorr).

Use of a different background gas could provide a means of reducing the condensation heat flux on the target. However, example calculations done with He as background gas indicated no significant improvement. The benefit of avoiding transfer of the latent heats to the target and of shielding the target by reflected He atoms was found to be counter-balanced by the relatively higher He molecular flux on the moving target (as compared to Xe) for the same pressure and temperature.

Radiation from the chamber wall exacerbates the situation depending on the surface reflectivity. For example, the maximum radiated heat flux from the chamber wall to the target in a 6-m radius chamber is 6000 W/m^2 for a wall temperature of only 545 K. An effort is underway to model the radiation effect in more detail including refraction, attenuation and reflection through the target constituent layers, and to better understand the effect of the optical properties of these layers. This will be described in a future report.

The presence of cold plasma remaining during target injection could also increase the heat flux due to ion recombination at the target surface. This is being addressed via a separate effort.

It is clear that the whole target thermal design should be revisited. In particular, the following questions should be addressed:

1. The thermal limit must be revisited. Is the triple point really the limit or should it be lower or higher than this? Would the presence of a very thin liquid DT layer cause enough perturbation as to affect the functioning of the target? Are there other limits such as possible stress fracture that should be considered?
2. Can the target be injected at a temperature lower than 18 K?
3. Can the target design and injection method be modified to provide more thermally robust target or more shielding during injection?

In addition to the effort on the more detailed radiation analysis and as part of its continuing effort in this area, UCSD proposes to start addressing these questions in collaboration with GA.

References

1. N. P. Siegel, "Thermal Analysis of Inertial Fusion Energy Targets," Master of Science Thesis, San Diego State University, May 2000.
2. R. Petzold, GA, personal communication. Also, DSMC code runs courtesy of GA, November 2001.
3. ANSYS 5.7, ANSYS Inc., Canonsburg, PA
4. J. G. Collier, Convective Boiling and Condensation, 2nd Edition, Mc Graw-Hill, New York, 1981.
5. R. F. Brown, D. M. Trayer, and M. R. Busby, "Condensation of 300-2500 K Gases on Surfaces at Cryogenic Temperatures," The Journal of Vacuum Science and Technology, Vol. 7, No. 1, 1969.